Int J Adv Manuf Technol (2017) 90:2453–2460
DOI 10.1007/s00170-016-9576-2

ORIGINAL ARTICLE

Mathematical modeling and machining parameter optimization for the surface roughness of face gear grinding

Xingzu Ming[1] · **Qin Gao**[1] · **Hongzhi Yan**[2] · **Jinhua Liu**[1] · **Cuijiao Liao**[1]

Received: 6 March 2016 / Accepted: 6 October 2016 / Published online: 17 October 2016

Abstract Face gear is an important part in the power transmission of helicopter, but its grinding is a difficult problem. In order to enhance the finishing machining surface quality of face gear, the mathematical formula of the residual height of motion trajectory of abrasive grains was obtained, and the model of grinding surface roughness of face gear was corrected. In addition, machining parameter optimization for grinding surface roughness on a five-axis blade grinding machine was investigated by orthogonal experiment method. The experiment results indicated that disk wheel spindle speed and feed velocity of the disk wheel are more significant effect factors among the three factors. The calculation results of model showed that the maximum error comparing with the experiment results is not more than 13.5 %, which suggests that the mathematical model is reasonable.

Keywords Face gear grinding · Disk wheel · Surface roughness · Mathematical modeling · Parameter optimization

Nomenclature

$dg_{\max}$	The maximum diameter of abrasive grains
dg_{avg}	The average diameter of abrasive grains
μ	The normal distribution of the mean
σ	Standard deviation in the normal distribution
H_i	The bump height of abrasive grains
M	The size of abrasive grains
Δ	An average spacing between two adjacent abrasive grains on the grinding wheel surface
V_g	The volume percentage of abrasive grain in grinding wheel
r_s	Radius of grinding wheel
N_p	The number of abrasive grains in the grinding wheel section per unit area AB
v_s	Disk wheel spindle speed
v_w	Disk wheel feed velocity
θ	Grinding wheel angle
ω	Grinding wheel angular velocity
L	The distance between O_1 and O in the X direction
r_1	The distance between the first grain and the grinding wheel center
r_2	The distance between the second grain and the grinding wheel center
ϕ	The angle difference between two adjacent abrasive grains
K	Grinding correction coefficient
η	Material relative removal coefficient
G_1, G_2	The code of two abrasive grains
Q	The intersection point of the trajectory of two abrasive grains
R	The residual height of motion trajectory of abrasive grains
Ra	The value of grinding surface roughness

✉ Xingzu Ming
83082907@qq.com

[1] School of Mechanical Engineering, Hunan University of Technology, Zhuzhou, Hunan 412007, China

[2] College of Mechanical and Electrical Engineering, Central South University, Changsha, Hunan 410083, China

1 Introduction

Face gear is an important element of power and motion transmission owing to its compact structure, light weight, large transmission ratio, and high load capacity, especially in the helicopter gearbox [1–3].

There are two kinds of manufacturing method for face gear: rough machining and finishing [4–6]. Grinding as a finishing machining method is a commonly used manufacturing technology and is an allowable application on face gear with hardened materials. But, face gear grinding is a very difficult problem because of the complex surface and machining precision, and so, it has attracted a lot of attention. Litvin et al. [7] put forward a precision grinding method for face gear by a worm wheel with a special shape. Beel et al. [8] proposed a CNC grinding machining method with a worm wheel. Other research [9, 10] also investagted the related work on grinding machining by worm wheels and designing the machining apparatus. They found that the complexity and wear of the worm wheel surface affects on the profile accuracy and machining efficiency of face gear. Tang et al. [11] studied the grinding principle of face gear using disk wheel and built a theoretical model of face gear based on the bevel gear grinding machine. Wang et al. [12] proposed a grinding method for face gear with CBN disk wheel, which can improve grinding precision. Guo et al. [13] presented a grinding method for face gears by CNC machines and built an envelope residual model for face gear. They provided some effective approaches for parameter selection to raise the precision and efficiency of face gear grinding. However, the related problems of surface roughness of face gear grinding have not been discussed.

The tooth surface roughness significantly influences corrosion resistance, fatigue, abrasion resistance, and the transmission quality of face gear; so, it is an important indicator evaluating the quality of face gear tooth surface. In this paper, face gear was ground on QMK50A blade grinding machine; a theoretical model of tooth surface roughness was established based on grinding track by Matlab software. The tooth surface roughness was considered as a target variable; the machining parameters were optimized by orthogonal experimental method.

2 Theoretical model

2.1 The assumptions and simplified conditions

Grinding surface roughness is generally impacted by grain distribution, size, the number of grains per unit area of the grinding wheel, and so on. As well as the cutting edges do not distribute in a perfect circle on the surface of the grinding wheel. In the process of face gear grinding, the surface roughness is mainly an effect by the residual height of grain trajectory because of the spatial curved surface of face gear [14]. In order to obtain the theoretical model of the residual height of grinding grain motion trace, we will establish the theoretical formula based on the following assumptions and simplified conditions:

(1) The formation method of the workpiece surface is pure cutting, namely, the surface uplift and plow are ignored.
(2) Excluding the effect of the abrasive wear of the grinding wheel and the vibration of machine.
(3) Assuming the same shape and uniform distribution of abrasive grains.
(4) Ignoring the elastic deformation of grinding wheel, etc.

2.2 The grinding wheel topography analysis

As we all known, abrasive grain sizes, the number of grains, and disk wheel grinding parameters have a great influence on surface roughness of grinding tooth surface. The abrasive grain bump height H_i of disk wheel obeys normal distribution [15]. When the abrasive grain size is M, the maximum diameter of grains can be expressed as Eq. 1 [16, 17]:

$$dg_{\max}(mm) = 1.52M^{-1} \tag{1}$$

The average diameter of grain can be expressed as Eq. 2:

$$dg_{avg}(mm) = 68M^{-1.4} \tag{2}$$

The bump height of abrasive grain H_i obeys (μ, σ^2) normal distribution, among,

$$u = dg_{avg} \tag{3}$$

And,

$$\sigma = \left(\mathrm{dg}_{\max} - \mathrm{dg}_{avg}\right)/3 \tag{4}$$

$$\Delta = 137.9M^{-1.4}\sqrt[3]{\frac{2\pi}{V_g}} \tag{5}$$

As shown in Fig. 1, the number of abrasive grains of the grinding wheel at section with per unit area AB is set to N_p [18]:

$$N_p \cdot \frac{\pi}{6} dg^3{}_{avg} = V_g/100 \cdot \left(1 \times dg_{avg}\right) \tag{6}$$

$$N_p = \frac{6V_g}{100\pi dg^2{}_{avg}} \tag{7}$$

2.3 Abrasive trajectory analysis

In order to facilitate the analysis, we simplify the process of face gear grinding. The relative motion of the grinding wheel along the helix is expanded as a straight line, and the

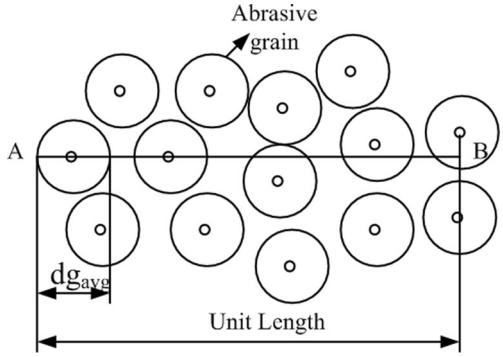

Fig. 1 Grinding wheel internal particle distribution

workpiece x–y coordinate system was established as shown in Fig. 2. The origin point is the tangency point of grinding wheel and the workpiece. The motion equation of grain G can be described as follows:

$$x = v_w t + \mathrm{r}_s \sin\theta \tag{8}$$

$$y = r_s(1-\cos\theta) \tag{9}$$

$$v_s t = r_s \theta \tag{10}$$

x and y can be obtained by the above expression.

$$x = r_s\left(\frac{v_w}{v_s} + 1\right) \tag{11}$$

$$y = \frac{1}{2} r_s \theta^2 \tag{12}$$

The grain trajectory equation can be obtained from the above two Eqs. 11 and 12.

$$y = \frac{r_s x^2}{2\left(r_s + \frac{v_w}{\omega}\right)^2} \tag{13}$$

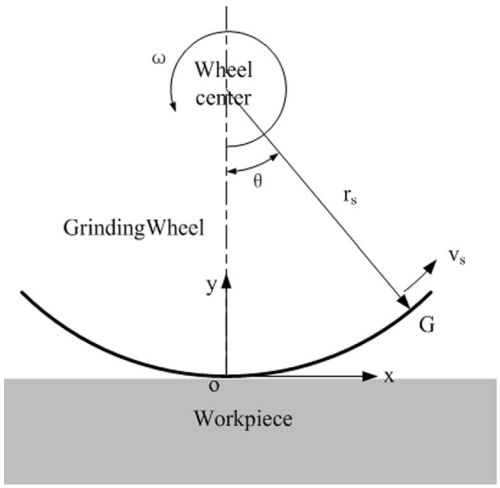

Fig. 2 Single particle track

By analyzing the movements of two adjacent grains, the intersection point of two-grain track was calculated. The local coordinate system (x_1, y_1) for the first grain G_1 was established as shown in Fig. 3; its origin point is coincident with the global coordinate system (x, y). We can conclude that the trajectory equation of the first grain G_1 [19]:

$$y_1 = \frac{r_1 x_1^2}{2\left(r_1 + \frac{v_w}{\omega}\right)^2} \tag{14}$$

$$y_2 = \frac{r_2 {x_1}^2}{2\left(r_2 + \frac{v_w}{\omega}\right)^2} \tag{15}$$

The time difference between the two grains can be expressed as Eq. 16.

$$\Delta t = \frac{L}{v_w} = \frac{r_s \phi}{v_s} \tag{16}$$

Among,

$$L = \frac{v_w}{v_s} r_s \phi = \frac{v_w}{\omega}\phi \tag{17}$$

Grain G_2 locus equation in the global coordinate system can be expressed as Eq. 18.

$$y + (r_1 - r_2) = \frac{r_2\left(x - \frac{v_w}{\omega}\phi\right)}{2\left(r_1 + \frac{v_w}{\omega}\right)^2} \tag{18}$$

In the global coordinate system, then, Eq. 19 is the trajectory equation of grains.

$$y + (r_i - r_1) = \frac{r_i\left(x - \frac{v_w}{\omega} i\phi\right)}{2\left(r_1 + \frac{v_w}{\omega}\right)^2} \tag{19}$$

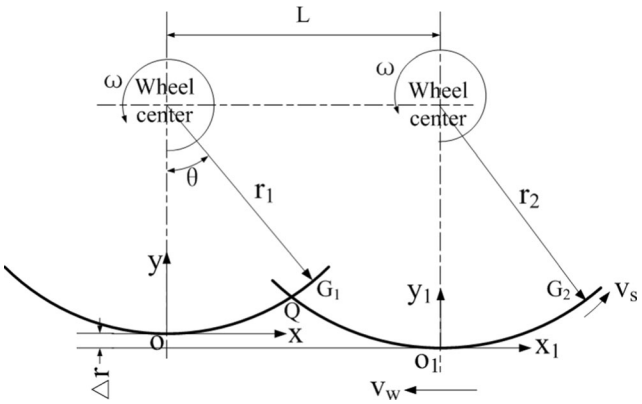

Fig. 3 The trajectory of adjacent two grains

Through Eqs. 15 and 18, the intersection point of the trajectory of two abrasive grains can be determined because of the same y value in the intersection point, then,

$$\frac{r_1 x^2}{2\left(r_1+\frac{v_w}{\omega}\right)^2}+(r_2-r_1)=\frac{r^2\left(x-\frac{v_w}{\omega}\phi\right)^2}{2\left(r_2+\frac{v_w}{\omega}\right)^2} \tag{20}$$

Put it into quadratic equation in X direction, then,

$$\left(\frac{r_2}{K_2}-\frac{r_1}{K_1}\right)x^2-2\frac{r_2 v_w}{K_2\omega}\phi x+\left[\frac{\left(\frac{v_w}{\omega}\phi\right)^2 r_2}{K_2}-2(r_2-r_1)\right]=0 \tag{21}$$

Among,

$$K_1=2\left(r_1+\frac{v_w}{\omega}\right)^2 \tag{22}$$

$$K_2=2\left(r_2+\frac{v_w}{\omega}\right)^2 \tag{23}$$

In the formula,

$$A=\left(\frac{r_2}{K_2}-\frac{r_1}{K_1}\right) \tag{24}$$

$$B=-2\frac{r_2 V_w}{K_2\omega} \tag{25}$$

$$C=\frac{\left(\frac{v_w}{\omega}\phi\right)^2 r_2}{K_2}-2(r_2-r_1) \tag{26}$$

The coordinates of intersection Q is obtained.

$$x_{1,2}=\frac{-B\pm\sqrt{B^2-4AC}}{2A} \tag{27}$$

The y coordinate of the intersection $y_{1,2}$.can be obtained by Eq. 27 and Eq. 19.

$$R=\sqrt{x_{1,2}^2+y_{1,2}^2} \tag{28}$$

Considering the plastic lateral uplift and tillage plow of the grinding surface, mechanical vibration, and so on, the theoretical model of surface roughness of grinding tooth is amended. Its correction value is [14]:

$$Ra=K\cdot R \tag{29}$$

$$K=\left(1+\sqrt{(1-\eta)/2}\right) \tag{30}$$

In this paper, the material of face gear is 18Cr2Ni4WA, the value of K is obtained by the literature and is 1.1 to 1.2 [20]. In abrasive cutting depth smaller, plastic larger, plow effect increases, K value the larger.

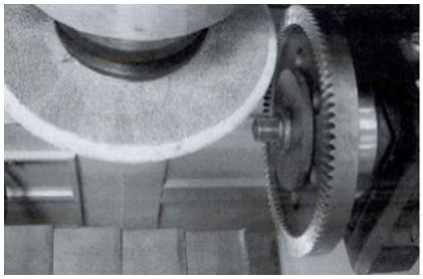

Fig. 4 The scene drawing of face gear grinding

3 Experiments and methods

3.1 Equipment and conditions

Grinding experiments were carried out on a QMK50A blade grinding machine with five-degrees of freedom. The machining has five numerically closed-loop controlled axes, Siemens 840D as a CNC system. The power of spindle motor is 13 kW, and the maximum spindle speed is 60,000 rpm. The scene diagram of face gear grinding is presented in Fig. 4. Al_2O_3 wheel was used to grind face gear. The details about the related parameters of face gear and grinding wheel are listed in Table 1 and Table 2, respectively. The tooth surface roughness was examined on Hommel Werke T800.

3.2 Experiment method

As we all know, there are a lot of effect factors of face gear grinding surface roughness. Based on the above analysis, we know that the residual height of grain trajectory, which is determined by the movement trajectory of grinding tooth surface and is affected by the geometry of tooth surface, the grinding process, and parameters, is a main effect factor of surface roughness of face gear grinding. In the process of face gear grinding, some factors are certain such as the material and the hardness of face gear and grinding fluid. In addition,

Table 1 Design parameters of face gear

Items	Values
Number of teeth of the face gear	60
Number of teeth of Pinion gear	23
Module	3.5 mm
Pressure angle	20°
Addendum coefficient	1.0
Dedendum coefficient	1.25
Crossed axis angle	90°
Outer radius of the face gear	120 mm
inner radius of the face gear	102.5 mm
Tooth width	17.5 mm
Gear helical angle	0

Table 2 The experimental conditions of grinding face gear

Items	Values
CNC gear grinding machine type	QMK50A
The diameter of the disk wheel	300 mm
Abrasive	white corundum (Al_2O_3)
The material of face gear	18Cr2Ni4WA
The heat treatment of face gear	Quenching, HRC56–63
The cooling liquid	Water-based grinding fluid

grinding of face gear is a final finishing machining method; the change range of grinding depth is little and not more than 0.02 mm. So, these factors can be regarded a non-significant variables. By contrast, the change range of disk wheel spindle speed, disk wheel feed velocity, and abrasive grain size is big. So, these three factors are regarded as effect factors in orthogonal experiment [21], by which the influence law of surface roughness for face gear grinding was researched.

In order to investigate the relationship between effect factors and surface roughness, each factor has 5 levels. **L**25 (5^3) orthogonal table was selected. The level values of each factor are listed in Table 3, and the machining parameters of each experiment are listed in Table 4. The accepted tooth surface roughness of each experiment is the mean value of five measurement values getting rid of the maximum and the minimum values.

4 Results and discussions

4.1 Range analysis of orthogonal experiment

This paper does not present the calculation processes of mean and range; the calculation results are listed in Table 5. k_i is the average of the experiment values of surface roughness in the i level. The order of the factors is listed according to the size of ranges. The larger range suggests the larger influence on the test result. The order of range shown in Table 5 is A (disk wheel spindle speed) >B (disk wheel feed velocity) >C (abrasive code), the range of A is close to that of B. The result indicates that the spindle speed and feed velocity of the disk wheel are the two main influence factors.

Table 3 Levels for three factors in **L**25 (5^3) orthogonal experiment design

Levels	Factors		
	Disk wheel spindle speed (rev/min) A	Disk wheel feed speed (m/min) B	Abrasive code (#) C
I	1300	1.6	60
II	1600	2.1	80
III	2000	2.6	100
IV	2500	4.0	120
V	3200	5.6	150

Table 4 Orthogonal experiment and results

Experiment no.	Real value			Surface roughness Ra (μm)	The percentage of calculation error (%)
	A	B	C		
1	1300	1.6	60	0.755	6.9
2	1300	2.1	80	0.556	9.9
3	1300	2.6	100	0.645	2.1
4	1300	4.0	120	0.770	2.0
5	1300	5.6	150	0.802	-5.0
6	1600	1.6	80	0.522	13.5
7	1600	2.1	100	0.554	4.2
8	1600	2.6	120	0.441	-12.2
9	1600	4.0	150	0.595	1.2
10	1600	5.6	60	0.832	-8.2
11	2000	1.6	100	0.390	-6.5
12	2000	2.1	120	0.385	7.2
13	2000	2.6	150	0.410	3.6
14	2000	4.0	60	0.702	-11
15	2000	5.6	80	0.714	2.9
16	2500	1.6	120	0.315	3.6
17	2500	2.1	150	0.310	3.9
18	2500	2.6	60	0.339	9.1
19	2500	4.0	80	0.602	-7.3
20	2500	5.6	100	0.624	-9.2
21	3200	1.6	150	0.295	5.6
22	3200	2.1	60	0.449	2.1
23	3200	2.6	80	0.395	-2.2
24	3200	4.0	100	0.462	-7.1
25	3200	5.6	120	0.570	8.5

Table 5 Range analysis of orthogonal experimental design for surface roughness

Levels	Factors		
	Disk wheel spindle speed (rev/min) A	Disk wheel feed velocity (m/min) B	Abrasive code (#) C
k_I	0.706	0.455	0.615
k_{II}	0.589	0.451	0.558
k_{III}	0.520	0.446	0.535
k_{IV}	0.438	0.626	0.496
k_V	0.434	0.708	0.482
Range (R)	0.272	0.262	0.133
Effect order		A>B>C	
Optimal level	A_5	B_3	C_5
Optimal case		A_5 B_3 C_5	

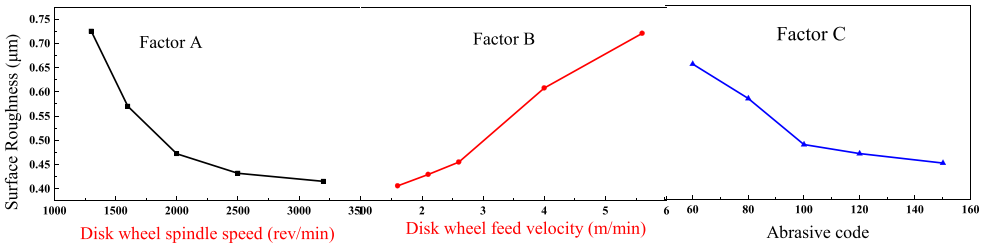

Fig. 5 The trend diagram of each factor for surface roughness

Table 6 Variance analysis of orthogonal experimental design for the surface roughness

Source	The sum of variances	Degree of freedom	Mean square error	F values	Sig.
Factor A	0.258798	4	0.0647	22.11189	Highly significant factor
Factor B	0.29852	4	0.07463	25.50573	Highly significant factor
Factor C	0.056142	4	0.014035	4.79679	Significant factor
Error	0.035112	12	0.002926		
Total	0.648572	24	0.027024		

Note: $F_{0.01}(4,12) = 5.41$, $F_{0.05}(4,12) = 3.26$, $F_{0.1}(4,12) = 2.48$

Optimal levels are determined by k_i values of each factor. The minimum surface roughness value is expected; so, A_5, B_3, and C_5 are the optimal levels for factors A, B, and C, respectively. Thus, we can get the optimal case $A_5B_3C_5$. But, the case is not exhibited in the orthogonal experiment table. In order to verify the reliability, another experiment was performed at the case $A_5B_3C_5$, namely, spindle speed, feed velocity, and abrasive code are 3200 rev/min, 2.6 m/min, and 150#, respectively. The surface roughness value gotten by the additive experiment is 0.293 μm and is smaller than 0.295 μm obtained at the case $A_5B_1C_5$.

The trend diagram of factors is exhibited in Fig. 5. As can be seen from the diagram, the surface roughness values decline with the spindle speed of the grinding wheel, their changes trend fellow the negative exponential function, which indicates that the higher spindle speed can improve surface roughness in a certain range. The surface roughness value increases with the feed velocity, and their relationship is nearly linear, which shows that the smaller feed velocity is conducive to obtain a good surface roughness. The trend diagram of factor C presents that the smaller abrasive grain is also easy to get a smaller surface roughness value.

4.2 Variance analysis of orthogonal experiment

Variance analysis is an effective method for finding out the significance factors and the interactive relationship between factors. We calculate the F value of each factor and consult Fisher's F_α (4,12) values at different probability values (e.g., $\alpha = 0.01, 0.05, 0.1$). The significance conclusion is drawn by comparing the calculation F value and the Fisher's F values. In this experiment, calculation F values of factor A and B are obviously larger than Fisher's F_α (4,12) values at any probability values; so, factors A and B are highly significant factors. The calculation F value of factor C is larger than $F_{0.05}(4,12)$ and $F_{0.1}(4,12) = 2.48$ and is smaller than $F_{0.01}(4,12) = 5.41$; so, factor C is also a significant factor. There is no detailed calculation process; the results are listed in Table 6.

4.3 Comparative analysis between experiment and calculation values

The comparative analysis between experiment values and calculation values was performed to examine the correctness of the theoretical model. The percentage of calculation relative error values are listed in Table 4. The maximum and minimum absolute percentage of the calculation relative error values are 13.5 and 1.2 %, respectively. From a statistical standpoint, the calculation error values basically follow normal distribution except for the range of −5~0 %, as shown in Fig. 6, which

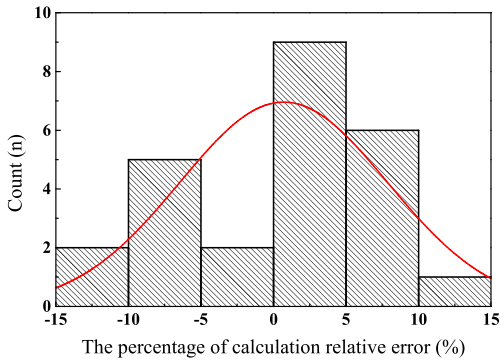

Fig. 6 The statistical curve of the calculation values

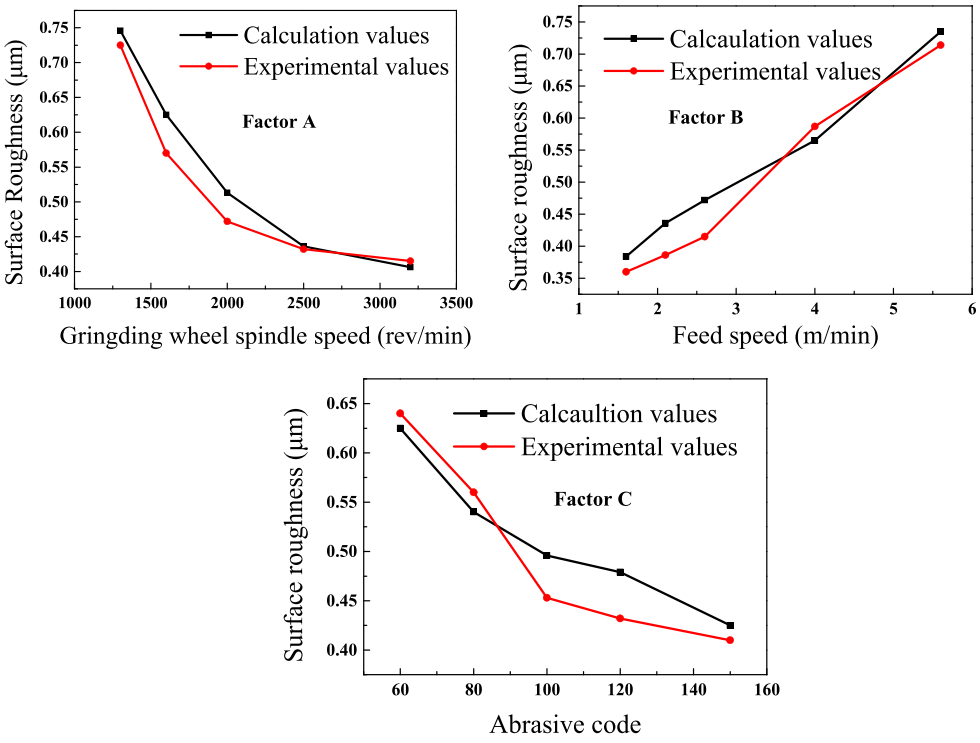

Fig. 7 The change curve of the calculation values for each factor

indicates that the theoretical model of tooth surface roughness of grinding face gear is accurate and credible.

The change curves of the calculation values for each factor are exhibited in Fig. 7. The variation tendencies of experimental and calculation values are similar. The deviation values between experimental and calculation values of factors A and B at levels 2 and 3 are larger than those of at the other levels (levels 1, 4, and 5). Similarly, the deviation values of factor C at levels 3 and 4 are larger than those of at levels 1, 2, and 5. These phenomena demonstrate that the theoretical model may have a best value range for each factor, which can direct the modification of the theoretical model.

5 Conclusions

In this paper, the theoretical model and orthogonal experiment were performed, and the following conclusions are found:

(1) The orthogonal experiment shows that disk wheel spindle speed and feed velocity are the main effect factors for surface roughness and $A_5B_3C_5$ is the most optimal experiment case, at which the obtained surface roughness is 0.293 μm.
(2) The theoretical model can basically reflect the real experiment case; the maximun absolute percentage of the calculation relative error is 13.5 % and is within the allowed error range.

Acknowledgments This work was financially supported by the National Natural Science Foundation of China (Grant Nos. 51375161, 51575533 and 51505141), and Hunan Provincial Natural Science Foundation of China (2015JJ5018).

References

1. Litvin F, Wang JC, Bossler R, Chen YJ, Heath G, Lewicki D (1994) Application of face-gear drives in helicopter transmissions. J Mech Des 116:672–676
2. Litvin F, Zhang Y, Wang JC, Bossler R, Chen YJ (1992) Design and geometry of face-gear drives. J Mech Des 114:642–647
3. Lin C, Cao XJ, Fan Y, Zeng D (2016) Pitch deviation measurement and analysis of curve-face gear pair. Measurement 81:95–101
4. Yang XY, Tang JY (2014) Research on manufacturing method of CNC plunge milling for spur face-gear. J Mater Process Technol 214:3013–3019
5. Tang J, Yang X (2016) Research on manufacturing method of planing for spur face-gear with 4-axis CNC planer. Int J Mach Tools Manuf 82:847–858
6. Wang YZ, Hou WL, Lan Z, Zhu CL (2016) Precision milling method for face-gear by disk cutter [J]. Int J Adv Manuf Tech:1–14. doi:10.1007/s00170-016-9189-9
7. Litvin FL, Fuentes A, Zanzi C, Pontiggia M, Handschuh RF (2002) Face-gear drive with spur involute pinion: geometry, generation by a worm, stress analysis. Comput Method Appl M 191:2785–2813
8. Beel K, Fisher D, Russell A, Folprecht G (2002) Face gear manufacturing method and apparatus. US Patent 6, 390, 894, B1

9. Gao J, Zhu R, Li Z (2011) Research on singularities of base worm thread surface for hobbing or grinding face gear. J Aerosp Power 26:2394–2400
10. Wang Y, Wu C, Ge X, Zhang L (2009) Basal worm-designing method of face-gear hob. J Beijing Univ Aeronaut Astronaut 35: 166–169 in Chinese
11. Tang JY, Yin F, Chen XM (2013) The principle of profile modified face-gear grinding based on disk wheel. Mech Mach Theory 70:1–15
12. Wang Y, Lan Z, Hou L, Zhao H, Zhong Y (2015) A precision generating grinding method for face gear using CBN wheel. Int J Adv Manuf Tech 79:1839–1848
13. Guo H, Peng X, Zhao N, Zhang S (2015) A CNC grinding method and envelope residual model for face gear. Int J Adv Manuf Tech 79:1689–1698
14. Xiu S, Li C, Cai G (2005) Modification for theoretical model of ground surface roughness. J Northeast Univ Nat Sci 26:770 in Chinese
15. Dai K, Villegas J, Shaw L (2005) An analytical model of the surface roughness of an aluminum alloy treated with a surface nanocrystallization and hardening process. Scr Mater 52:259–263
16. Kwak JS, Sim SB, Jeong YD (2006) An analysis of grinding power and surface roughness in external cylindrical grinding of hardened SCM440 steel using the response surface method. Int J Mach Tools Manuf 46:304–312
17. Cao YL, Guan JY, Li B, Chen XL, Yang JX, Gan CB (2013) Modeling and simulation of grinding surface topography considering wheel vibration. Int J Adv Manuf Tech 66:937–945
18. Davim JP, Gaitonde V, Karnik S (2008) Investigations into the effect of cutting conditions on surface roughness in turning of free machining steel by ANN models. J Mater Process Technol 205:16–23
19. Zhang KL, Wei JJ (2010) Analysis and simulation of numerical control grinding spherical roughness based on MATLAB [J]. Modul Mach Tool & Auto Manuf Tech 3:007 in Chinese
20. Nguyen T, Butler D (2005) Simulation of surface grinding process, part 2: interaction of the abrasive grain with the workpiece. Int J Mach Tools Manuf 45:1329–1336
21. Du JP (2008) Research about optimization of grinding process based on fuzzy synthetic evaluation. Coal Mine Machinery 49(7): 55–57 in Chinese